Relaxation Time in Globular Clusters

J Kalnins
Gravitational Collapse Group
Submitted: March 13, 2020

The encounter-relaxation model for evolution of globular clusters, as proposed by Chandrasekhar (1942), was tested by the means of multiple direct N-Body simulations, ranging from 100 to 1000 particles of mass varying from $10^{30} - 10^{35}$kg in a spherical space of $r_{\max} \approx 30$pc. The data was observed to fit the theory as a function of both particle mass and number of particles, but due to the initial conditions of the simulation, the characteristic half-mass radius was shown to be dependent on the number of particles, which introduced uncertainty into the results for relaxation time. The Coulomb logarithm $\ln\Lambda$ was found to be proportional to $\ln\gamma N$ with $\gamma = 0.113(2)$, and the relationship of relaxation time with mass was found to be $t_{rh} \propto m^{-0.502(1)}$. Mass segregation under the Spitzer condition was studied, but was limited due to hardware limitations.

I. INTRODUCTION

A. A Brief History

Astrophysical systems are hard to study, both because of their size and the timescales involved in their evolution. We cannot test their evolution and structure directly. Therefore, computer models are a vital tool for studying astronomy. The foundations of N-body gravitational simulation were laid in 1941 by Holmberg [1] who simulated the interactions of a 37-body system by replacing the gravitational forces with the intensity of light from lightbulbs, as both follow an r^2 force law.

In the 1960s, computer simulation of N-body systems began on primitive computers (von Hoerner [2] describes programming using hole-punched tape, debugging using a hole-punch and scissors!). In 1963, Aarseth [3] built the first edition of the NBODY-X codes to simulate $25 \leq N \leq 100$ particles, studying the evolution of galaxies in a cluster. These codes continue to develop, incorporating new techniques to make best use of the huge computing power available.The limits on direct N-body calculations now reaching the order of 10^4 particles [4].

B. Gravitational Dynamics

The gravitational force acting on a particle i can be described by the equation:

$$\frac{\partial^2 \vec{r_i}}{\partial t^2} = \vec{F_i} = -\sum_{j \neq i} G \frac{m_i m_j (\vec{r_i} - \vec{r_j})}{|\vec{r_i} - \vec{r_j}|^3} \tag{1}$$

This calculation is valid for the non-relativistic regime - that is, where high-mass objects do not come too close to one another. Outside of this regime, General Relativity must be applied, but this is beyond the scope of this report. For any defined set of initial conditions (a set of particles with mass, position and velocities), the solution to the differential equation is unique. However, it can only be determined analytically for two bodies. For more bodies, a numerical approach must be used. This can be done directly (by computing the force between each pair of particles and integrating to find the velocity & position of particles) or indirectly by considering the gravitational field due to many particles at once, and describing this with an equation dependent on the macroscopic properties of the system.

C. Globular Clusters & Relaxation

Coined by Herschel in 1789 [5], globular clusters are groups of a few hundred thousand stars which are strongly gravitationally bound (giving their spherical shape). They orbit galaxies and their half-mass radii are of the order of 10pc. There are some 150 globular clusters in the Milky Way [6]. Theoretical models for their evolution have been proposed based on observed clusters, but because we cannot observe them over astronomical timescales or from any perspective other than our terrestrial one, these models must be tested using other means.

The timescale on which globular clusters evolve dynamically can be derived theoretically by considering the sum of all gravitational interactions on a star in the cluster. Chandrasekhar (1942) [7] and Spitzer (1987) [6] both derive the following equation with slightly different methods, but achieve the same result. The full derivation is not reproduced here. The change in stellar velocity due to a gravitational interaction is calculated (under various assumptions) then expanded to consider the average change on all stars in the cluster. When this velocity change becomes large, the cluster is considered to have evolved dynamically. This timescale is known as the relaxation time:

$$t_r = \alpha \frac{v^3}{Nm^2 G \ln\Lambda} \tag{2}$$

Here, α is a constant (Spitzer [6] gives $\alpha = 0.065$), v the average velocity of the stars, N the number of stars, m their average mass, and G the Newtonian gravitational constant. $\ln\Lambda = \ln(b_{\max}/b_{\min})$ is the Coulomb logarithm, the ratio of the minimum & maximum radius of encounters. This parameter, originally used in plasma physics, is introduced in order to provide finite limits of an integral over particle separation.

Calculating t_r for globular clusters gives times of the order of $10 - 1000$MYr. Calculating the relaxation time for galaxies gives $t_r >> t_H$ ($t_H = 1/H_0$ is the Hubble time, an approximation for the age of the universe), which implies that factors other than gravitational relaxation are important in the evolution of galaxies. Without other factors, they would not have

undergone much evolution on the timescale of the universe, which is not consistent with observation. They are therefore unsuitable for direct N-body simulations.

Eq. (2) is not necessarily useful, because of ambiguity in how the parameters are defined. In particular, v isn't well defined in the context of the simulation. In order to avoid this issue, we apply the Virial energy theorem which describes systems in dynamical equilibrium ($2K + U = 0$) to find v^3. In addition, because the outer radius of a cluster is difficult to define, we consider consider the half-mass radius r_h (the radius of the sphere in which half the cluster mass is contained). Using this, we can derive the half-mass relaxation time t_{rh} to be:

$$t_{rh} = \beta \frac{N^{1/2} r_h^{3/2}}{m^{1/2} G^{1/2} \ln \Lambda} = \beta \frac{N}{\ln \Lambda} \left(\frac{r_h^3}{GM} \right)^{1/2} \tag{3}$$

$M = Nm$ is the cluster mass, and β is a constant which Spitzer found to be 0.138.

The Coulomb logarithm ($\ln \Lambda$) is the subject of some debate. Spitzer [6] proposes that $\Lambda = \gamma N$, with $\gamma = 0.4$. Giersz & Heggie [8] found $\gamma = 0.11$ in a series of N-body simulations. There is some debate over this term, and in particular it's inclusion in the equation - indeed, over the entire encounter-relaxation model (cf. Hamilton et al. (2018) [9]).

II. SIMULATION TECHNIQUES

A. Integration Scheme

Calculating the force on each particle is simple, but computationally slow. The number of calculations can in fact be halved by using equal & opposite forces (i.e. $\vec{F}_{AB} = \vec{F}_{BA}$). However, this step still requires $\mathcal{O}(N^2)$ computational time, and is the main bottleneck of the code's speed.

When the forces on all particles are known, their positions must be updated. This process requires some consideration, as standard integration techniques have errors which compound over time [10]. This error can be improved by applying a symplectic integration scheme - that is, one which conserves the canonical nature of the Hamiltonian of the system. In an ideal situation, when applied in reverse (i.e. with timestep $-\Delta t$), the initial conditions of the system would be returned. In this experiment, a Leapfrog integration scheme was applied (Fig. 1). This system was chosen for two factors - firstly, as previously mentioned, the symplectic nature of the scheme conserves energy, and secondly this method requires few calculations per step, so does not cost much computation time. The steps are shown below, for calculating the velocity & position of the ith particle at the $(n+1)$th timestep, assuming $\vec{F}_i^{\,n}$ is known:

$$\begin{aligned} \vec{v}_i^{\,n+1/2} &= \vec{v}_i^{\,n-1/2} + \vec{F}_i^{\,n} \Delta t / m_i \\ \vec{r}_i^{\,n+1} &= \vec{r}_i^{\,n} + \vec{v}_i^{\,n+1/2} \Delta \end{aligned} \tag{4}$$

The symplectic nature of the integration scheme can be used to test how large numerical errors become, by running

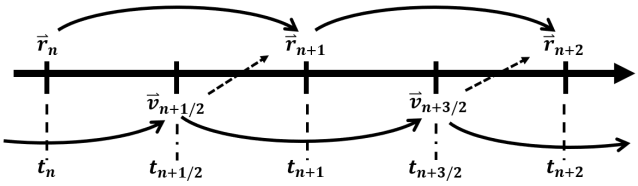

FIG. 1: The Leapfrog integration method. Dotted arrows show dependence of $\vec{r}^{\,n}$ on $\vec{v}^{\,n-1/2}$. Reproduced from McMillan's diagram [10].

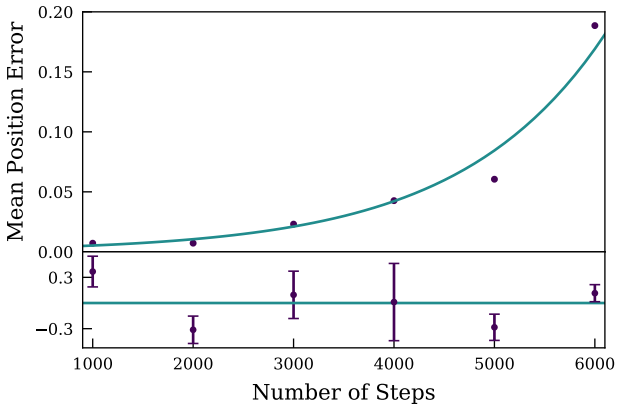

FIG. 2: Graph showing the dependence of mean error in initial position calculation on number of timesteps. Blue line demonstrates an exponential relationship to the number of steps; although there are significant errors, due to the individual simulations having varying starting positions.

a simulation backwards from its final conditions to its initial conditions, then comparing the difference between the two. Long timesteps and large numbers of heavy particles affect this difference as numerical errors build up more over time. Simulations with the same initial conditions (particle mass & number) were run for varying numbers of timesteps. These simulations were reversed from their final positions and run back to their starting positions. The mean difference in position from the initial conditions was then calculated. The results are shown in Fig. 2.

B. Softening

Real objects will collide when the distance between them comes close to zero. However, in the simulation, particles are assumed to be point-like. This causes issues when the particles' calculated positions become close to one another over the course of a timestep, as the force between them (and therefore their velocities) tends to infinity. This becomes particularly awkward when a single timestep places particles very close to one another, quickly generating forces of huge magnitude and therefore massive velocities (many times the speed of light) which are obviously not physically possible, let alone

realistic. This is solved by introducing a softening parameter ϵ into the force calculation (Eq. (1)):

$$\vec{F_i} = -\sum_{j \neq i} G m_i m_j \frac{(\vec{r_i} - \vec{r_j})}{[|\vec{r_i} - \vec{r_j}|^2 + \epsilon^2]^{3/2}} \tag{5}$$

This parameter limits the fraction to $1/\epsilon^3$ when $(\vec{r_i} - \vec{r_j}) \to 0$, thus avoiding errors in the code resulting from large forces and velocities. For the purposes of this simulation, ϵ was initially set to be $\epsilon = 0.1 r_{\max}/N^{1/3}$, in order to be proportional to the minimum spacing between particles at $t = 0$.

C. Initial Conditions

To simulate globular clusters, initial conditions must be chosen to match observations. Several simplifications were made to these conditions in order to allow simulation. The validity of these assumptions will be discussed later in the report.

The density of globular clusters has been often modelled using a Plummer sphere [11], which has a roughly constant central density then falls off rapidly outside some characteristic radius. This radius was assumed to be approximately the half-mass radius, and the simplification was made that inside the half-mass radius, particle number density is constant; outside this volume the density is negligible.

To generate particles in a sphere, a Poisson disk distribution was used. A modified version of Bridson's algorithm [12] was used to generate points in a 3D cube, then deselect any that were outside a given radius or whose distance to any other points was less than $d_{\min}$ (This places points as if each is a sphere with radius $d_{\min}/2$). This selection method generates a uniform distribution where no two particle begin at close separation. This choice was made to avoid initial strong encounters in the simulation. These strong encounters do occur in astrophysics (for example, Proxima Centauri orbits α Centauri at 0.02pc [13]) but since our choice of ϵ already somewhat precludes accurate study of so-called 'hard' binaries, they were ignored. They may still occur during evolution, but beginning without any binaries avoids issues.

The masses of the particles were set to a given value, as the decision was made to study constant-mass systems. The initial velocity was set to zero. This initially leaves the system out of equilibrium, but as the system should collapse, this is acceptable.

III. RESULTS

A. Initial Models

Simulations were run with masses ranging from 10^{31}-10^{35}kg with N ranging from 100-1000. The virial energy of these simulations (Fig. 3) showed a peak corresponding to a collapse followed by a slow expansion. It was theorised

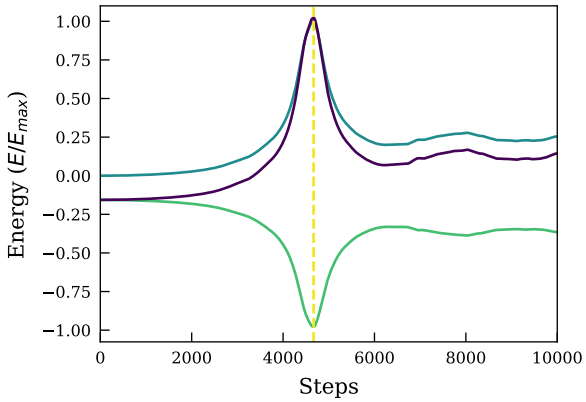

FIG. 3: Normalised kinetic (blue), gravitational potential (red) and virial (purple) energy against time for a 1000 particle system. The yellow line marks the collapse time of $t = 4.504 \times 10^{15}$s. The virial energy after collapse is slightly above the expected zero, due to the softening parameter used to calculate the potential energy.

that this collapse corresponded to the relaxation time so this timescale was studied.

Eq. (3) suggests that t_{rh} is affected by both particle mass and particle number. The data collected was fitted to two different models to reflect this using a multi-parameter least-squares minimisation technique (χ^2 minimisation). During data collection, some departure from the predicted model was observed. To account for this, two three-parameter models were proposed:

$$t_{rc,I} = A_I m^{-B_I} \frac{N}{\ln C_I N} \tag{6a}$$

$$t_{rc,II} = A_{II} m^{-B_{II}} N^{-C_{II}} \tag{6b}$$

Model I (Eq. (6a)) follows the theoretical prediction. A_I is the pre-factor, and the predicted values of the other parameters are $B_I = 1/2$ and $C_I = 0.11$, coming from Eq. (3) and previous simulations [8] respectively. Model II (6b) is deliberately more vague than I, with no expected values for any of the parameters.

Model I was inaccurate, with a very large value of $\chi^2_{\nu,\min}$. However, this uncertainty in the model was mainly due to the parameter A_I which had a very large error of almost 50%. The value of A_I is essentially unimportant, as it is dependent on the initial conditions. However, values for B_I and C_I had smaller errors; $B_I = 0.50(7)$ and $C_I = 0.113(2)$. B_I is in agreement with the equation prediction within its' error, and C_I is in agreement with [8], but the overall poor fit suggests that these results are of questionable significance. The parameter A_I, when compared to Eq. (3), should be of the value $A_I = r_h^{3/2}/G^{1/2} \propto r_h^{3/2}$. In theory, when the total radius is held constant, r_h should be constant, regardless of particle number, because the particle distribution has constant density. However, the uncertainty in A_I suggests that this is not necessarily the case. Further to this, the assumption that the observed spike in energy correlates to the relaxation time may be incorrect.

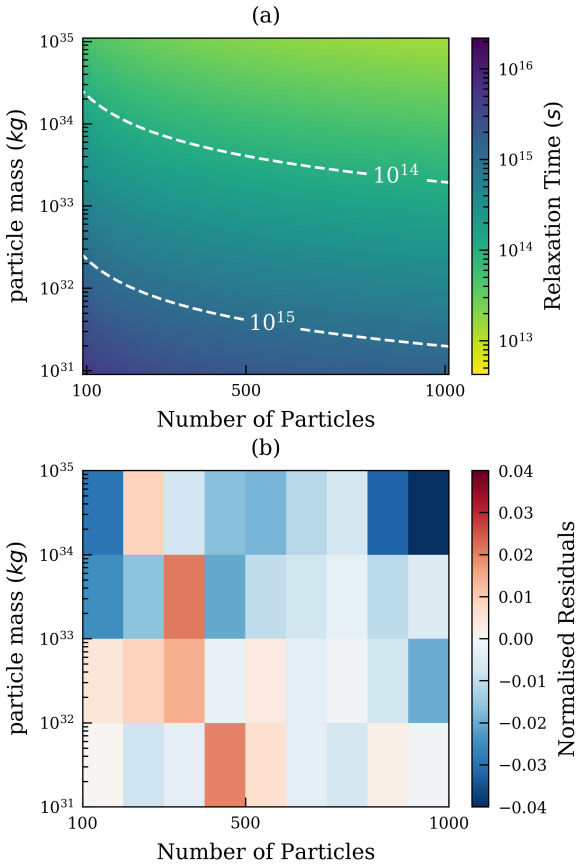

FIG. 4: (a) shows a heatmap of the fit to model II for t_{rh}. The measured fit was $t_c = 2.0(2) \times 10^{31} m^{-0.502(1)} N^{-0.530(1)}$, with $\chi^2_{\nu,\min} = 4.63$. (b) shows the residuals of the collapse times for the simulation groups which were used to collect data for the fit. Simulations were run, ranging from 100 to 1000 particles with particle masses ranging from $10^{31} - 10^{35}$kg.

Model II, however, gave $\chi^2_{\nu,\min} = 4.63$ and had a mean normalised residual of $\bar{e}_t = 0.0146$, suggesting a good fit was found (Shown in Fig. 4). The parameters B_{II} & C_{II} are most interesting, as they describe the dependence of the results on m and N. The minimisation algorithm reports $B_{II} = 0.502(1)$, and $C_{II} = 530(1)$. This suggests good agreement with the mass-dependence of $m^{1/2}$, and the value of C_{II} suggests that N does not follow a simple power-law, which is in agreement with the theory. Once again, the value of A_{II} has a large error ($\alpha_A \sim 0.1 A_{II}$).

The collapse times measured were on the scale of $10 - 100$MYr. This agrees with previous observations of physical clusters [14]. This implies that the simulation does form an accurate model of globular clusters, despite its' issues and simplifications.

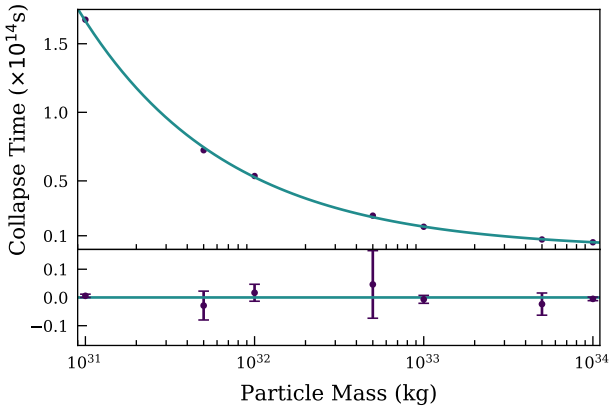

FIG. 5: Collapse time of simulated clusters for varying particle masses. The least-squares fit of the average collapse time is shown as the blue line, of the form $t = Am^{-1/2}$, with $A = 5.27(1) \times 10^{29}$. Error-bars for each point are shown in green.

B. Constant Particle Number model

Both models discussed had large uncertainty in the parameter A. Therefore, more simulations were run. As both models suggested the $m^{-1/2}$ dependence was correct, a constant particle number was chosen, and particle mass was varied in order to study the parameter A.

The model used was of the form $t_{rc} = Am^{-1/2}$, and $A = 5.27(1) \times 10^{29}$ was calculated. A good fit was found, as $\chi^2_{\nu,\min} = 0.485$. Fig. 5 shows the fit against the data. This result implies that the uncertainty in A_I is not due to the changing value of m, and suggests that when N changes, uncertainty is introduced into the value of A_I. Studying the terms present in Eq. (3) can give insight into why this error appears. Firstly, we assume that β may be discounted as a constant (Both Chandrasekhar and Spitzer's derivations suggest this to be the case [6, 7]). Then, the only factors left are those of N and m which have already been considered, and the value of r_h. Therefore, this value was examined further.

C. Half-Mass Radius Modelling

The initial assumption that $r_{\max} \approx r_h$ was not supported by the simulation data. Re-analysing data collected in previous simulations offers some insight into the reasoning for this. Firstly, Eq. (3) was rearranged to find an expression for r_h. The measured collapse times were used to calculate a predicted value for r_h and this was compared to our assumption of $r_{\max}$. The results suggest that r_h is independent of m but follows a power law with respect to N as $r_h \propto N^{-1/2}$. The data shown in Fig. 6 suggests the relationship $r_h/r_{\max} = 3.38(5) N^{-0.484(2)}$.

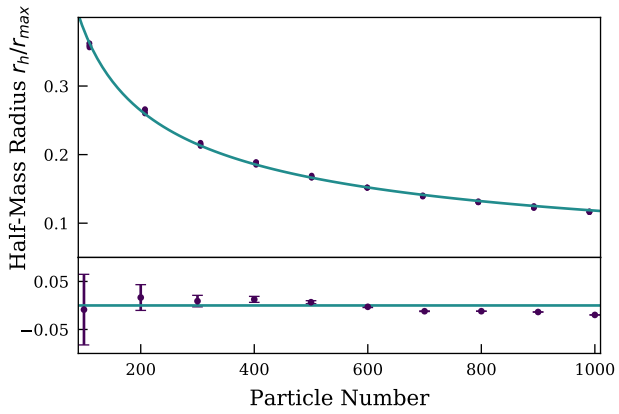

FIG. 6: Graph showing the dependence of relaxation time (Eq. (3)) on particle number, normalised to the maximum radius of the particle positions $r_{\max} = 10^{18}$m. The data demonstrates the relationship of $r_h = AN^{-1/2}$ with $A = 3.38(5)$.

IV. DISCUSSION

A. Relaxation Time

The results collected demonstrate that the equation for relaxation time is an appropriate model. In particular, strong evidence was found for the Coulomb Logarithm $\ln \Lambda$ affecting the results. This supports the accepted theory, although this theory is suggested to be a simplification of the physical reality [9, 15, 16]. No evidence was found to support this - however, the resolution of the system may be such that this behaviour is not observable. A large-scale reproduction of these simulations may provide insight into this by allowing for a more thorough treatment of the system itself. In particular, a variable timestep (allowing for smaller timesteps between particles with small separation) would increase the accuracy of the results to physical systems; currently the ϵ-softening method applied is less accurate but required for usable computation times.

The particle-mass dependence that was predicted was also found to be accurate. This was as expected, as this element of the formula has not been questioned in the same way as the Coulomb logarithm, because fewer assumptions that affect the mass value were made during its' derivation [7]. Nevertheless, these results suggest that assuming all particles have a constant mass of some value is a valid assumption to make in modelling clusters. A brief study of a split-mass system was also done, in order to test the phenomenon of mass segregation, predicted by Spitzer [17]. He predicts that the heavier star population will collapse, due to energy equipartition being impossible, unless the following condition is satisfied:

$$S = \frac{M_2}{M_1}\left(\frac{m_2}{m_1}\right)^{3/2} < 0.16 \tag{7}$$

Where M_1 is the total mass of the light fraction, and M_2 the total mass of the heavy fraction. m_1 and m_2 are the masses of the individual light and heavy particles respectively. When $S < 0.16$, the heavy fraction and light fraction should be able to exist in equipartition. If $S > 0.16$, the heavy fraction will contract to form an extremely dense core. Simulations were run with $0.07 < S < 0.65$ but the expected behaviour was not observed. Fig. 7 shows that there is little difference in the radii for the light and heavy sections, other than the expected smaller radii (b) due to the heavier total mass and resulting larger gravitational potential energy. The 5% radius was chosen in order to ignore escaping light particles.

The lack of expected difference was due to the low particle numbers resulting in noisy data and the softening parameter stopping hard binaries forming. The low particle numbers meant that the heavy fraction has only a few stars. The inner 5% of the light fraction suffers from this issue also, leading to a high noise factor (seen in the lack of a smooth curve in the light fractions in Fig. 7). The softening parameter forces binaries to become less strongly bound than they would in reality. This means that the forces that would bind the heavy fraction together are decreased, causing the expected contraction to not occur.

B. Half Mass Radius

In spite of the accuracy of parts of the results as discussed, the overall agreement with theory was poor, due to the dependence of r_h on the number of particles, as shown in Fig. 6. Theoretically, if the particle number density ρ is constant in the sphere, then $M_h \propto V_h = 2\pi r_{\max}^3/3$. We can use this fact to find that, in theory, $r_h = r_{\max}/\sqrt[3]{2}$. Since the simulation initial conditions were built so that this condition (constant ρ) was satisfied, another explanation must be found for the dependence of r_h on N. This explanation lies in considering the system energy.

In deriving Eqs. eqs. (2) and (3), the assumption was made that the system initially begins in equilibrium, which is not the case for the simulation that was used. The approximation was made that the initial kinetic energy $K = 0$. It is clear that $U \propto N$, so in fact as N increases, the system moves further and further from virial equilibrium ($2K + U < 0$). This means that the system will undergo a collapse initially to a more compact state. During this time, the kinetic energy will increase as the particles accelerate towards the centre of mass (on average). Therefore, a time will be reached where the more compact state is in equilibrium. Systems with larger N require more kinetic energy to balance the potential energy, so must collapse further in order to supply more energy, resulting in a smaller radius when they reach equilibrium.

This smaller radius is the radius which should actually be used when calculating a (correct) value of t_{rh}. The dependence of this radius on N explains the issues observed with the model fit and explains the large uncertainty observed in the pre-factor.

In order to correct for this in future, when the particle positions are generated, an isotropic velocity distribution should be applied to the particles in order to supply kinetic energy to

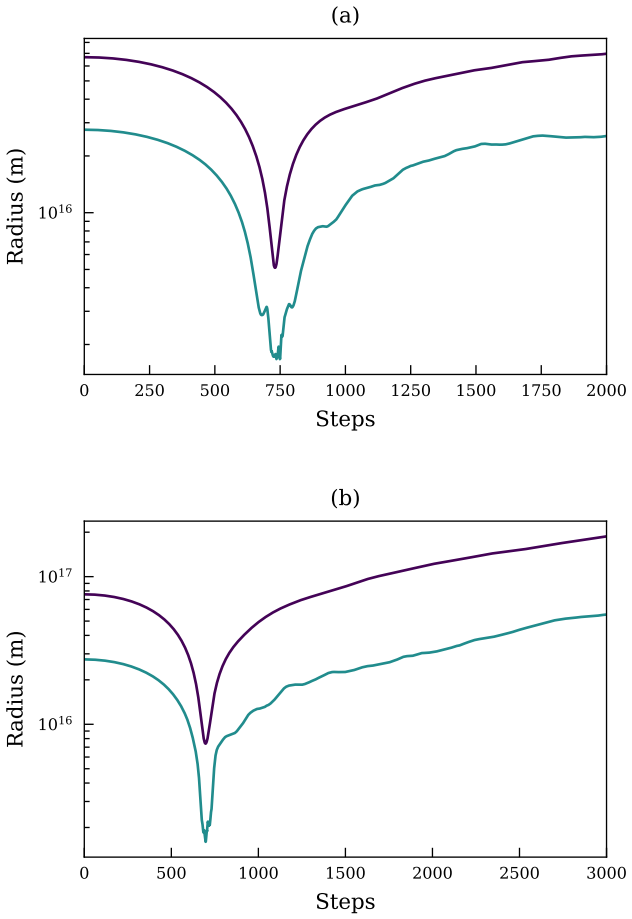

FIG. 7: Plots showing the average radius of the heavy particle fraction (purple) compared to the radius of the nearest 5% of the light particle fraction (blue). (a) shows a simulation with $S = 0.0716$ and (b) shows a simulation with $S = 0.629$. Very little difference in the overall shape of the graphs is observed. In particular, (a) does not show the expected slow decrease of the heavy fraction that Spitzer predicts.

balance the system energy. This would also allow for study of rotating clusters as opposed to those supported by random motions. Initial attempts made at this were limited by the difficulty of selecting a random velocity dispersion to give the correct total energy whilst also preserving an isotropic cluster motion.

V. CONCLUSION

The theory that two-body relaxation drives the long-term evolution of globular clusters was tested and found to be accurate. Particularly, the dependence of relaxation time on particle mass was found to be accurate ($t_{rh} \propto m^{0.502(1)}$), and the approximation of the Coulomb logarithm as $\ln \gamma N$ was found to be valid, with $\gamma = 0.113(2)$.

The initial condition of zero particle velocity was shown to be a poor approximation when particle number increased; the cause for this is believed to be the imbalance of kinetic and potential energy. The constant particle mass approximation was shown to fit the predicted model, suggesting that approximating globular clusters as spheres of particles with constant number density and mass is valid.

Further research could involve studying mass segregation under the Spitzer condition, and apply a velocity dispersion in order to balance the cluster's initial energy and enable the study of rotating clusters.

REFERENCES

[1] E. Holmberg, On the clustering tendencies among the nebulae. ii. a study of encounters between laboratory models of stellar systems by a new integration procedure., The Astrophysical Journal **94**, 385 (1941).
[2] S. von Hoerner, How it all started, in Dynamics of star clusters and the Milky Way, Vol. 228 (2001) p. 11.
[3] S. J. Aarseth and F. Hoyle, Dynamical evolution of clusters of galaxies, i, Monthly Notices of the Royal Astronomical Society **126**, 223 (1963).
[4] S. J. Aarseth, From nbody1 to nbody6: The growth of an industry, Publications of the Astronomical Society of the Pacific **111**, 1333 (1999).
[5] W. Herschel, Xx. catalogue of a second thousand of new nebulæ and clusters of stars; with a few introductory remarks on the construction of the heavens, Philosophical transactions of the Royal Society of London , 212 (1789).
[6] L. S. Spitzer, Dynamical Evolution of Globular Clusters (Princeton University Press, 1987).
[7] S. Chandrasekhar, Principles of stellar dynamics (University of Chicago Press, 1942).
[8] M. Giersz and D. C. Heggie, Statistics of n-body simulations– i. equal masses before core collapse, Monthly Notices of the Royal Astronomical Society **268**, 257 (1994).
[9] C. Hamilton, J.-B. Fouvry, J. Binney, and C. Pichon, Revisiting relaxation in globular clusters, Monthly Notices of the Royal Astronomical Society **481**, 2041 (2018).
[10] S. McMillan, The leapfrog integrator (1998).
[11] H. C. Plummer, On the problem of distribution in globular star clusters, Monthly notices of the royal astronomical society **71**, 460 (1911).
[12] R. Bridson, Fast poisson disk sampling in arbitrary dimensions., SIGGRAPH sketches **10**, 1278780 (2007).
[13] P. Kervella, F. Thévenin, and C. Lovis, Proxima's orbit around α centauri, Astronomy & Astrophysics **598**, L7 (2017).
[14] C. J. Peterson and I. R. King, The structure of star clusters. vi. observed radii and structural parameters in globular clusters., The Astronomical Journal **80**, 427 (1975).
[15] J.-B. Fouvry and B. Bar-Or, Relaxation in self-gravitating systems, Monthly Notices of the Royal Astronomical Society **481**, 4566 (2018).
[16] J. Heyvaerts, J.-B. Fouvry, P.-H. Chavanis, and C. Pichon, Dressed diffusion and friction coefficients in inhomogeneous multicomponent self-gravitating systems, Monthly Notices of the Royal Astronomical Society **469**, 4193 (2017).
[17] L. Spitzer Jr, Equipartition and the formation of compact nuclei in spherical stellar systems, The Astrophysical Journal **158**, L139 (1969).